

ARTICLE—50<sup>th</sup> ANNIVERSARY SPECIAL ISSUE

## EP2 Receptor Signaling Regulates Microglia Death

Yujiao Fu, Myung-Soon Yang, Jianxiong Jiang,<sup>1</sup> Thota Ganesh, Eunhye Joe, and Raymond Dingledine

Department of Pharmacology, Emory University School of Medicine, Atlanta, Georgia (Y.F., M.-S.Y., J.J., T.G., R.D.); Neurology Department, Xiangya Hospital, Hunan, China (Y.F.); and Department of Pharmacology, Ajou University School of Medicine, Suwon, Korea (M.-S.Y., E.J.)

Received January 30, 2015; accepted February 20, 2015

### ABSTRACT

The timely resolution of inflammation prevents continued tissue damage after an initial insult. In the brain, the death of activated microglia by apoptosis has been proposed as one mechanism to resolve brain inflammation. How microglial death is regulated after activation is still unclear. We reported that exposure to lipopolysaccharide (LPS) and interleukin (IL)-13 together initially activates and then kills rat microglia in culture by a mechanism dependent on cyclooxygenase-2 (COX-2). We show here that activation of the E prostanoid receptor 2 (EP2, PTGER2) for prostaglandin E<sub>2</sub> mediates microglial death induced by LPS/IL-13, and that EP2 activation by agonist alone kills microglia. Both EP2 antagonists and reactive oxygen scavengers block microglial death induced by either LPS/IL-13 or EP2 activation. By contrast, the homeostatic induction of heme oxygenase 1 (Hmox1) by LPS/

IL-13 or EP2 activation protects microglia. Both the Hmox1 inducer cobalt protoporphyrin and a compound that releases the Hmox1 product carbon monoxide (CO) attenuated microglial death produced by LPS/IL-13. Whereas CO reduced COX-2 protein expression, EP2 activation increased Hmox1 and COX-2 expression at both the mRNA and protein level. Interestingly, caspase-1 inhibition prevented microglial death induced by either LPS/IL-13 or low (but not high) concentrations of butaprost, suggestive of a predominantly pyroptotic mode of death. Butaprost also caused the expression of activated caspase-3 in microglia, pointing to apoptosis. These results indicate that EP2 activation, which initially promotes microglial activation, later causes delayed death of activated microglia, potentially contributing to the resolution phase of neuroinflammation.

### Introduction

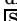
Microglia, the major innate immune cell type in the brain, respond to neuronal injury or prolonged seizures by transitioning from a resting to a classically activated state characterized by increased phagocytotic activity and release of numerous inflammatory molecules (Ransohoff and Cardona, 2010). Prompt resolution of inflammation once the original stimulus has been quenched is important to prevent a state of chronic inflammation

that can lead to additional tissue injury and dysfunction. The processes by which inflammation is resolved in peripheral tissues such as lung are known to include apoptotic death of activated macrophages (Marriott et al., 2006). Like macrophages, activated microglia can be driven into apoptosis, which has been proposed to contribute to a return to the resting state (Yang et al., 2002). Mechanisms controlling microglial apoptosis are incompletely characterized but important to protect the brain from entering a state of chronic inflammation.

A number of pathways appear to control the entry of activated microglia into cell death programs. One microglial apoptotic pathway involves Toll-like receptor 4-mediated formation of interferon  $\beta$  and subsequent engagement of caspases 11 and 3 (Jung et al., 2005). Another is triggered by formation of interleukin (IL)-13 by activated microglia (Shin et al., 2004), followed by induction of Jun kinase and consequent induction of

This work was supported by the National Institutes of Health [Grants R21-NS074169, U01-NS058158, and P20-NS080185], NARSAD Young Investigator Grant, and the National Institutes of Health National Institute of Neurological Disorders and Stroke [Grants K99/R00-NS082379].

<sup>1</sup>Current affiliation: Division of Pharmaceutical Sciences, James L. Winkle College of Pharmacy, University of Cincinnati, Cincinnati, Ohio.  
dx.doi.org/10.1124/mol.115.098202.

 This article has supplemental material available at molpharm.aspetjournals.org.

**ABBREVIATIONS:** AH6809, 6-isopropoxy-9-oxoxanthene-2-carboxylic acid; BHA, butylated hydroxyanisole; calcein-AM, calcein-acetoxymethyl ester; CO, carbon monoxide; CoPP, cobalt protoporphyrin; CORM, carbon monoxide-releasing molecule; CT, cycle threshold; FBS, fetal bovine serum; FRET, fluorescence resonance energy transfer; IL, interleukin; LPS, lipopolysaccharide; MEM, minimum Eagle's medium; NAC, *N*-acetyl cysteine; ONO-8711, 6-[(2*R*,3*S*)-3-[[[4-chloro-2-methylphenyl]sulfonyl]amino]methyl]bicyclo[2.2.2]oct-2-yl]-5*Z*-hexenoic acid; PBS, phosphate-buffered saline; qRT-PCR, quantitative real-time polymerase chain reaction; ROS, reactive oxygen species; SC-51089, 8-chloro-2-[1-oxo-3-(4-pyridinyl)propyl]hydrazide-dibenz[*b,f*]1,4-oxazepine-10(11*H*)-carboxylic acid, monohydrochloride; SE, status epilepticus; TG4-155, (*E*)-*N*-(2-(2-methyl-1*H*-indol-1-yl)ethyl)-3-(3,4,5-trimethoxyphenyl)acrylamide; TG6-10-1, (*E*)-*N*-(2-(2-(trifluoromethyl)-1*H*-indol-1-yl)ethyl)-3-(3,4,5-trimethoxyphenyl)acrylamide; TG7-170, *N*-(2-(2-methyl-1*H*-indol-1-yl)ethyl)-4-morpholinobenzamide.

cyclooxygenase-2 (COX-2). The resulting synthesis of prostaglandin E<sub>2</sub> (PGE<sub>2</sub>) causes microglial death (Yang et al., 2006). IL-13 is a canonical type 2 cytokine produced by many cell types that induces a state of alternative activation in macrophages and microglia (Van Dyken and Locksley, 2013). In classically activated microglia, IL-13 also opposes the induction of a major antioxidant protein, heme oxygenase 1 (Hmox1), and the resulting oxidative stress might contribute to development of the apoptotic state of microglia (Liu et al., 2010).

We were intrigued by results supporting the notion that enhanced death of activated microglia caused by IL-13 potentially involves activation of E prostanoid receptor 2 (EP2) receptors (Yang et al., 2006). Endogenously activated by PGE<sub>2</sub>, EP2 is a G<sub>α<sub>s</sub></sub>-coupled receptor that signals by cAMP formation, and in some cases via β-arrestin (Chu et al., 2014). The activation of Epac by cAMP underlies much of the immunomodulatory role of EP2 in classically activated microglia (Quan et al., 2013). Here we ask the following: 1) whether a selective EP2 antagonist prevents microglial cell death triggered by IL-13 and lipopolysaccharide (LPS); 2) whether EP2 influences the production of Hmox1 protein in activated microglia; 3) whether apoptosis and/or pyroptosis contributes to microglial death caused by EP2 activation; and 4) whether generation of reactive oxygen species (ROS) contributes to microglial death caused by IL-13 and LPS or by EP2 activation. The results indicate a powerful role for EP2 activation in autoregulatory death of microglia.

## Materials and Methods

**Reagents and Solutions.** LPS, carbon monoxide-releasing molecule (CORM) tricarbonyldichlororuthenium (II) dimer, bilirubin, FeSO<sub>4</sub>, Ac-YVAD-cmk, *N*-acetyl cysteine (NAC), and butylated hydroxyanisole (BHA) were purchased from Sigma-Aldrich (St. Louis, MO). Recombinant rat granulocyte-macrophage colony-stimulating factor (GM-CSF) and Z-WEHD-FMK were from R&D Systems (Minneapolis, MN). Recombinant rat IL-13 was from Peprotech (Rocky Hill, NJ). Cobalt protoporphyrin (CoPP) was from Porphyrin Products (Logan, UT). Butaprost, 17-phenyl trinor PGE<sub>2</sub> ethyl amide, and ONO-8711 (6-[(2*R*,3*S*)-3-[[[(4-chloro-2-methylphenyl)sulfonyl]amino]methyl]bicyclo [2.2.2]oct-2-yl]-5*Z*-hexenoic acid) were from Cayman Chemical Co. (Ann Arbor, MI). SC-51089 (8-chloro-2-[1-oxo-3-(4-pyridinyl)propyl]hydrazide-dibenz[*b,f*][1,4]oxazepine-10(1*H*)-carboxylic acid, monohydrochloride) was from Enzo Life Sciences (Farmingdale, NY). Minimum Eagle's medium (MEM), fetal bovine serum (FBS), and penicillin-streptomycin were from Gibco (Life Technologies, Grand Island, NY). HEPES was from GE Healthcare Hyclone (Logan, UT). Calcein-acetoxymethyl ester (calcein-AM) and ethidium homodimer-1 (Etd-1) for measurement of cell death were from Molecular Probes (Eugene, OR). The novel EP2 antagonists TG4-155 [(*E*)-*N*-(2-(2-methyl-1*H*-indol-1-yl)ethyl)-3-(3,4,5-trimethoxyphenyl)acrylamide], TG7-170 [*N*-(2-(2-methyl-1*H*-indol-1-yl)ethyl)-4-morpholinobenzamide], and TG6-10-1 [(*E*)-*N*-(2-(2-(trifluoromethyl)-1*H*-indol-1-yl)ethyl)-3-(3,4,5-trimethoxyphenyl)acrylamide] were synthesized in our laboratory.

**Microglial Cell Culture.** Pregnant Sprague-Dawley rats were from Charles River Laboratories (Wilmington, MA). Primary microglia were prepared from the cortex of 1- to 3-day-old Sprague-Dawley rats as described previously (Quan et al., 2013). In brief, cortical tissue was carefully freed from blood vessels and meninges, triturated, and washed. Cortical cells were cultured in MEM, 10% FBS with penicillin-streptomycin, plus 2 ng/ml GM-CSF for 10–14 days, during which medium was changed every 2–3 days. Microglia were then separated from the underlying astrocytic monolayer by gentle agitation. The cell pellet was resuspended in MEM, 5% FBS with penicillin-streptomycin, but lacking GM-CSF and plated on cell culture plates (Corning, Corning, NY). Nonadherent cells were removed after 30–60 minutes by

changing the medium, and then adherent microglia were incubated for 24 hours in culture medium before being exposed to drugs. Such cultures consist of >95% Iba1-positive microglia.

**Seizure Model and Drug Administration.** Male C57BL/6 mice (8–12 weeks old) from Charles River were housed under a 12-hour light/dark cycle with food and water ad libitum. To minimize peripheral side effects of pilocarpine, mice were injected with methylscopolamine and terbutaline (2 mg/kg each in saline, i.p.). After 15–30 minutes, pilocarpine (280 mg/kg in freshly prepared saline, i.p.) was injected to induce status epilepticus (SE). Control mice received methylscopolamine and terbutaline but no pilocarpine. Seizures were classified as previously described (Borges et al., 2003; Jiang et al., 2012, 2013): 0, normal behavior—walking, exploring, sniffing, grooming; 1, immobile, staring, jumpy, curled-up posture; 2, automatisms—repetitive blinking, chewing, head bobbing, vibrissae twitching, scratching, face-washing, “star-gazing”; 3, partial body clonus, occasional myoclonic jerks, shivering; 4, whole-body clonus, “corkscrew” turning and flipping, loss of posture, rearing and falling; 5 (SE onset), nonintermittent seizure activity; 6, wild running, bouncing, tonic seizures; 7, death. Mice underwent SE for 1 hour, and SE was then terminated by pentobarbital (30 mg/kg in saline, i.p.). After 3 hours, mice were randomized and received three doses of vehicle (10% dimethylsulfoxide, 50% PEG 400, and 40% ddH<sub>2</sub>O) or TG6-10-1 (5 mg/kg, i.p.) at 4, 21, and 30 hours after SE onset. Mice were fed moistened rodent chow, monitored daily, and injected with 5% dextrose in lactated Ringer's solution (0.5 ml, s.c.) (Baxter Healthcare, Deerfield, IL) when necessary. One day and 4 days after SE, groups of mice were euthanized under deep isoflurane anesthesia and perfused with phosphate-buffered saline (PBS) to wash blood out of the brain. Hippocampal tissues were then collected for measuring mRNA levels. All experiments were approved by the Institutional Animal Care and Use Committee of Emory University (Atlanta, GA) and conducted in accordance with its guidelines. Every effort was made to minimize animal suffering.

**Live and Dead Cell Assay.** Viability of microglia was assessed by double-labeling of cells with 2 μM calcein-AM and 4 μM Etd-1. Cells were counted using a Zeiss Axio Observer A1 fluorescence microscope (Zeiss, Oberkochen, Germany) and judged as being alive or dead from their color and shape by eye. Cells that were stained only red by Etd-1, or stained both green and red, or stained very bright green with a small round shape were counted as dead cells, whereas cells that were stained only green by calcein-AM and were not small, round, and bright were counted as live cells. In each condition, 600–900 cells were counted in eight fields from two different wells. Some of the data were analyzed in a blinded fashion (in Figs. 2A and 6A), and an excellent correlation was found between the scores from two independent raters of 28 images (Pearson's correlation = 0.97); one of the raters in this test was unaware of the treatment conditions.

**Quantitative Real-Time Polymerase Chain Reaction.** Total RNA from microglia culture or mouse hippocampus was isolated using TRIzol (Invitrogen, Life Technologies) with the PureLink RNA Mini Kit (Invitrogen, Life Technologies). RNA concentration and purity were measured by A260 value and A260/A280 ratio, respectively. First-strand cDNA synthesis was performed with 1 μg of total RNA, 200 units of SuperScript II Reverse Transcriptase (Invitrogen, Life Technologies), and 0.25 μg of random primers in a reaction volume of 20 μl at 42°C for 50 minutes. The reaction was terminated by heating at 70°C for 15 minutes. Quantitative real-time polymerase chain reaction (qRT-PCR) was performed by using 8 μl of 50× diluted cDNA, 0.4 μM primers, and 2× B-R SYBR Green SuperMix (Quanta BioSciences, Gaithersburg, MD) with a final volume of 20 μl in the iQ5 Multicolor Real-Time PCR Detection System (Bio-Rad Laboratories, Hercules, CA). Cycling conditions were as follows: 95°C for 2 minutes followed by 40 cycles of 95°C for 15 seconds and then 60°C for 1 minute. Melting-curve analysis was used to verify single-species polymerase chain reaction products. Fluorescent data were acquired at the 60°C step. The geometric mean of the cycle thresholds (CTs) for β-actin, glyceraldehyde-3-phosphate dehydrogenase, and hypoxanthine phosphoribosyltransferase-1 was subtracted from the CT measured for each gene of interest to yield ΔCT. Samples without cDNA template served as the negative controls.

Primers used for qRT-PCR were as follows:  $\beta$ -actin, forward 5'-CCAACCGTGAAAAGATGACC-3' and reverse 5'-ACCAGAGGCATACAGGGACA-3'; glyceraldehyde-3-phosphate dehydrogenase, forward 5'-GGTGAAGGTCGGTGTGAAC-3' and reverse 5'-CCTTGACTGTGC-CGTTGAA-3'; hypoxanthine phosphoribosyltransferase-1, forward 5'-GGTCCATTCCATGACTGTAGATTTT-3' and reverse 5'-CAATCAAGACGTTCTTTCCAGTT-3'; rat Hmox1, forward 5'-ACGAGGTGGGAGGTACTCAT-3' and reverse 5'-GCAGCTCCTCAAACAGCTCAA-3'; mouse Hmox1, forward 5'-GGAAATCATCCCTTGACGC-3' and reverse 5'-TGTTTGAAGTGGTGGGGCT-3'; and rat caspase-1, forward 5'-GAGCTTCAGTCAGGTCCATCA-3' and reverse 5'-AGGTCAACATCAGCTCCGAC-3'.

**Time-Resolved Fluorescence Resonance Energy Transfer cAMP Assay.** cAMP levels in microglia were measured with a homogeneous time-resolved fluorescence resonance energy transfer (FRET) method (Cisbio Bioassays, Codolet, France), as described by Quan et al. (2013). The assay is based on generation of a strong FRET signal upon the interaction of two molecules: an anti-cAMP antibody coupled to a FRET donor (cryptate) and cAMP coupled to a FRET acceptor (d2). Endogenous cAMP produced by cells competes with labeled cAMP for binding to the cAMP antibody and thus reduces the FRET signal, so the decrease of FRET signal indicates the increase of endogenous cAMP production. Briefly, microglia were seeded into 384-well plates in 30  $\mu$ l of complete medium (6000 cells/well) and grown overnight. Then cells were incubated with vehicle or 100 ng/ml of LPS for 24 hours. The medium was thoroughly withdrawn, and 10  $\mu$ l of Hanks' balanced salt solution (GE Healthcare Hyclone) plus 20  $\mu$ M rolipram was added into the wells to block phosphodiesterase. The cells were incubated at room temperature for 30 minutes and then treated with different concentrations of butaprost for 40 minutes. The cells were lysed in 10  $\mu$ l of lysis buffer containing the FRET acceptor cAMP-d2, and 1 minute later another 10  $\mu$ l of lysis buffer with anti-cAMP-cryptate was added. After a 60- to 90-minute incubation at room temperature, the time-resolved FRET signal was detected by an Envision 2103 multilabel plate reader (PerkinElmer Life Sciences, Waltham, MA) with laser excitation at 337 nm and dual emissions at 665 and 590 nm for d2 and cryptate, respectively. The FRET signal in Fig. 1 was scaled between its maximum and minimum levels.

**Western Blot.** After being seeded in six-well plates (500,000 cells/well), rat microglia received various treatments for indicated times and the cells were lysed on ice in RIPA buffer (Thermo Scientific, Waltham, MA) containing a mixture of protease and phosphatase inhibitors (Roche Applied Science, Penzberg, Germany). The lysate was centrifuged (12,000g, 15 minutes, 4°C), and protein concentration in the supernate was measured by Bradford assay (Thermo Fisher Scientific). The supernates (30  $\mu$ g of protein each) were resolved by 12.5% SDS-PAGE and electroblotted onto polyvinylidene fluoride membranes (Millipore, Billerica, MA). Membranes were blocked with 5% nonfat milk at room temperature for 2 hours, then incubated overnight at 4°C with primary antibodies: rabbit anti-Hmox1 (1:1000) (Santa Cruz Biotechnology, Dallas, TX), rabbit anti-caspase-1 (1:200) (Santa Cruz Biotechnology), goat anti-IL-1 $\beta$  (1:2000) (R&D Systems),

or mouse anti- $\beta$ -actin (1:16,000) (Abcam, Cambridge, MA). This procedure was followed by incubation with horseradish peroxidase-conjugated secondary antibodies (1:3000) (Santa Cruz Biotechnology) at room temperature for 2 hours. The blots were developed by enhanced chemiluminescence (Thermo Fisher Scientific).

**Immunocytochemistry.** Primary rat microglia were seeded in 24-well plates (100,000 cells/well) with coverslips on the bottom of each well. The coverslips were precoated with poly-L-lysine (0.01%) (Sigma-Aldrich). After incubation with drugs, cells were rinsed with ice-cold PBS; fixed with 4% paraformaldehyde for 20 minutes; washed three times with PBS; blocked for 2 hours in PBS, 10% goat serum, and 0.2% Triton X-100; and incubated overnight with the primary antibody, rabbit anti-cleaved caspase-3 (1:300) (Cell Signaling Technology, Danvers, MA). After washing three times with PBS and 0.2% Triton X-100, the cells were incubated with Alexa Fluor goat anti-rabbit (1:1000) (Molecular Probes) for 1 hour at room temperature. The cells were washed three times with PBS, and nuclei were counterstained with 4',6-diamidino-2-phenylindole (Vectashield Mounting Medium with DAPI; Vector Laboratories, Burlingame, CA) for 30 minutes. Fluorescence images were acquired using a Zeiss Axio Observer A1 fluorescence microscope. In control experiments, the cells were processed in a similar manner except the primary antibodies were omitted. All negative controls showed no staining (data not shown).

**Hmox1 Activity Assay.** Hmox1 enzyme activity was measured as previously described (Kutty and Maines, 1982). Cytosolic extracts were prepared as described by Devereaux et al. (1997). Briefly, rat liver was homogenized with ice-cold buffer A [20 mM HEPES (pH 7.5), 10 mM KCl, 1.5 mM MgCl<sub>2</sub>, 1 mM EDTA, and 1 mM dithiothreitol], washed twice, and pelleted by centrifugation. Cell pellets were resuspended in one volume of buffer A, incubated for 30 minutes on ice, and disrupted by 20 passages through a 26-gauge needle. Cell extract supernatant was recovered after centrifuging at 100,000g for 1 hour at 37°C. Microsomes from harvested cells were added to a reaction mixture containing NADPH (0.8 mM), rat liver cytosol (2 mg) as a source of biliverdin reductase, the substrate hemin (10  $\mu$ M), glucose 6-phosphate (2 mM), and glucose-6-phosphate dehydrogenase (0.2 U). The reaction was carried out in the dark for 1 hour at 37°C, and terminated by the addition of 500  $\mu$ l of chloroform. Hmox1 activity is shown as picomoles of bilirubin per milligram of protein per 60 minutes.

**Statistics.** Data are shown as mean  $\pm$  S.E.M.;  $n$  = number of independent experiments with each condition typically run in duplicate or triplicate, except Fig. 1, where the means of  $n$  = 3 or 4 technical replicates are shown in a single experiment. Comparisons are made by analysis of variance with correction for multiple comparisons as noted in the figure legends, or by one-sample  $t$  test in Figs. 1A and 7D.

## Results

**Activation of EP2 Receptors Underlies Microglial Death Induced by LPS/IL-13.** We have previously reported that COX-2 inhibitors prevent the death of rat microglia that

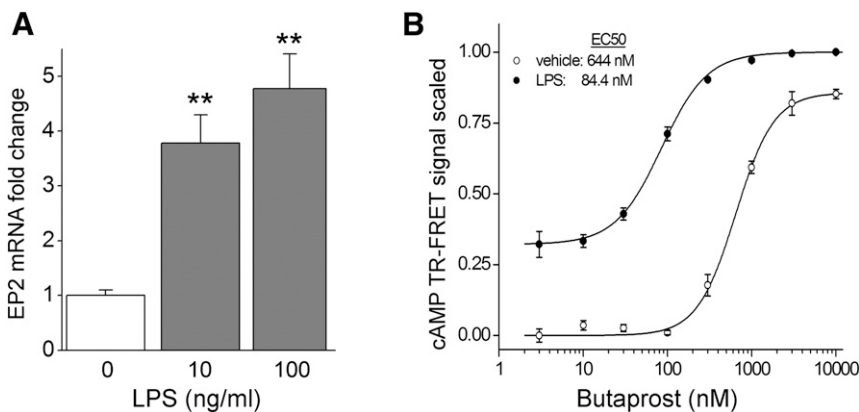


**Fig. 1.** Expression and activity of EP2 receptors in primary rat microglia. (A) Rat microglia were incubated with vehicle or 10 or 100 ng/ml of LPS for 24 hours, and mRNA levels were measured by qRT-PCR. The mRNA changes were normalized to the mean of the control group. Data were analyzed by one-sample  $t$  test with Bonferroni correction. Data are expressed as mean  $\pm$  S.E.M. (error bars);  $n$  = 5. \*\* $P$  < 0.01 versus control. (B) Rat microglia were incubated with vehicle or 100 ng/ml of LPS for 24 hours, followed by addition of different concentrations of butaprost for 2 hours. Cellular cAMP levels were evaluated by a time-resolved (TR) FRET assay. LPS caused a shift to the left in the butaprost concentration-response curve. Data points represent mean  $\pm$  S.E. (error bars) from a single experiment run in triplicate. This experiment was repeated with essentially the same results.

occurs several days after exposure to a combination of IL-13 and the inflammatory trigger LPS, and that a nonselective EP1/EP2 antagonist (AH6809, 6-isopropoxy-9-oxoxanthene-2-carboxylic acid) reduced cell death (Yang et al., 2006). COX-2 is dramatically upregulated and leads to PGE<sub>2</sub> synthesis during inflammation (Murakami et al., 2000; Quan et al., 2013). PGE<sub>2</sub> activates four different G protein-coupled receptors designated EP1, EP2, EP3, and EP4 (Narumiya et al., 1999). Cultured rat microglia were reported to express EP1, EP2, and EP4, but not the EP3 receptor subtype (Caggiano and Kraig, 1999; Shi et al., 2010). We confirmed the presence of EP2 receptors by qRT-PCR, and interestingly, we found that incubation with LPS (10 or 100 ng/ml) for 24 hours dose-dependently increased EP2 mRNA level in rat microglia (Fig. 1A). Further, to explore whether LPS alters the response of microglia to the EP2 agonist butaprost, we incubated rat primary microglia cultures with vehicle or 100 ng/ml of LPS for 24 hours followed by addition of different concentrations of butaprost for 2 hours. Butaprost activates EP2 to increase intracellular cAMP in rat microglia. Cellular cAMP levels were evaluated by a time-resolved FRET assay (Jiang et al., 2010) (Fig. 1B). LPS at 100 ng/ml produced an 8-fold shift to the left in the concentration-

response curve of butaprost, reducing its EC<sub>50</sub> from 644 nM in resting microglia to 84.4 nM in LPS-activated microglia.

To explore which prostaglandin receptor is involved in regulating microglial death, we examined the effects of selective EP1 and EP2 antagonists (Jiang et al., 2012) and agonists on microglial death. Butaprost selectively activates EP2, whereas 17-phenyl trinor PGE<sub>2</sub> activates EP1 and EP3 and increases intracellular [Ca<sup>2+</sup>] in rat astrocytes with an EC<sub>50</sub> of 69 nM (Kiriya et al., 1997). TG4-155 and TG7-170 are selective EP2 antagonists synthesized in our laboratory (Ganesh et al., 2014a,b) (Fig. 2A), and SC-51089 and ONO-8711 are selective EP1 antagonists (Hallinan et al., 1996; Watanabe et al., 1999). Both EP2 antagonists reduced LPS/IL-13-induced microglial death, whereas high concentrations of EP1 antagonists caused an insignificant reduction of cell death (Fig. 2, B and C). The observed trend for reduction of microglial death caused by EP1 antagonists might be explained by weak inhibition of EP2 receptors or a small contribution of EP1 receptor signaling. Additionally, the EP2 agonist butaprost itself dose-dependently induced rat microglial death, and this was reduced by both EP2 antagonists, but the EP1 agonist 17-phenyl trinor PGE<sub>2</sub> at 2 μM did not influence microglia cell viability (Fig. 2, D–F). Those

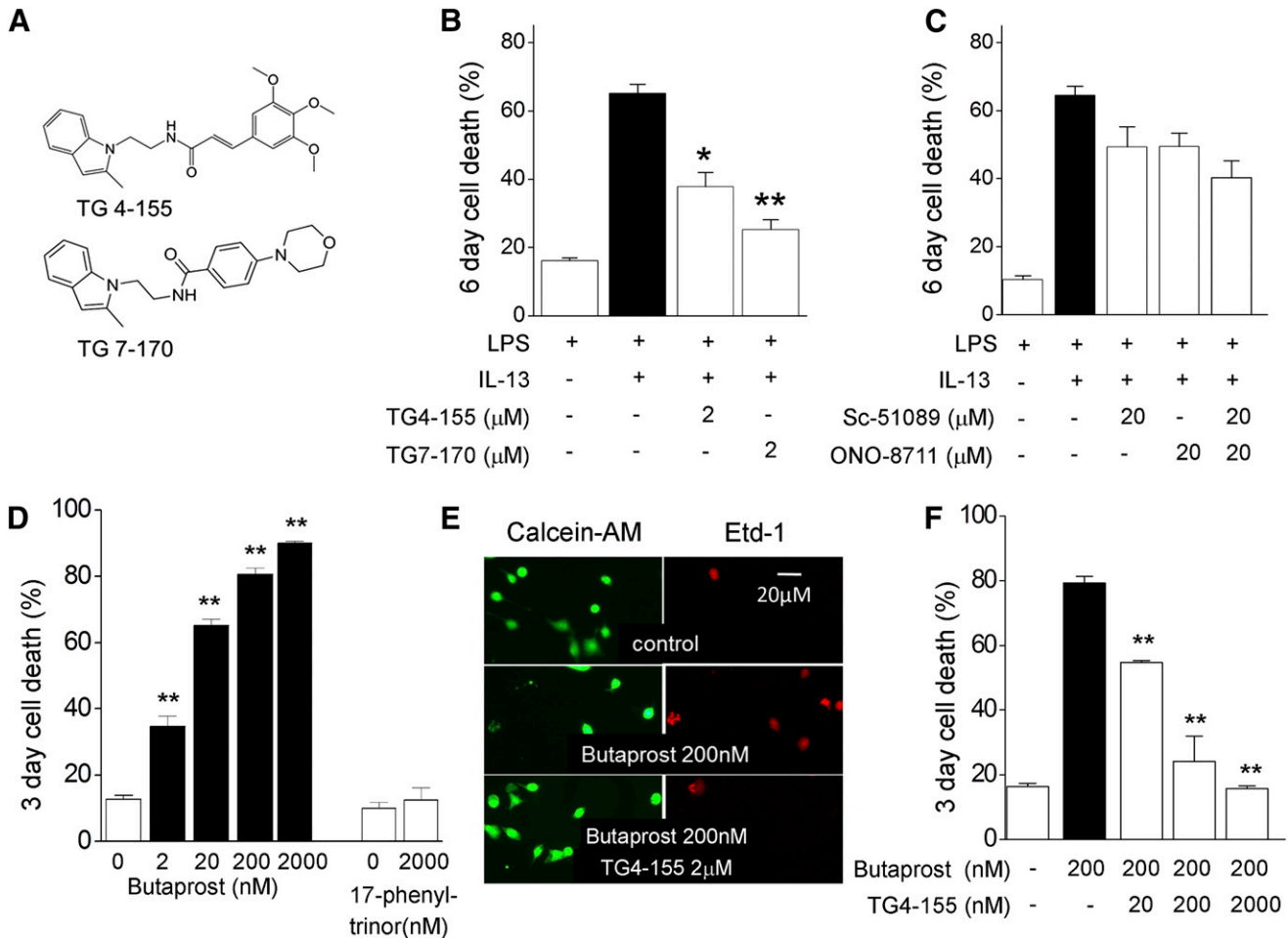


**Fig. 2.** EP2 activation produced cell death in both resting and activated microglia. (A) The structure of EP2 antagonists TG4-155 and TG7-170. (B and C) Rat microglia were pretreated with antagonists for EP2 (TG4-155 or TG7-170) (B) or EP1 (SC-51089 or ONO-8711) (C) receptors for 4 hours, followed by addition of 10 ng/ml of LPS and 20 ng/ml of IL-13 for 6 days. Cell death was determined by staining with calcein-AM and Etd-1. *n* = 4–6. (D) Microglia were incubated with vehicle or agonists of EP1 (17-phenyl trinor) or EP2 (butaprost) receptors for 3 days. Cell death was determined by staining. *n* = 3–6. (E and F) Microglia were pretreated with vehicle or indicated concentrations of the EP2 antagonist TG4-155 for 2 hours, followed by 200 nM butaprost for 3 days. Cell death was determined by staining. Representative images are shown. *n* = 3–6. Data were analyzed by one-way analysis of variance with Dunnett's test. Data are shown as mean + S.E. (error bars). \**P* < 0.05; \*\**P* < 0.01.

data together indicate that EP2 receptors are induced by microglial activation, and that EP2 activation contributes to microglial death that is produced by prolonged exposure to LPS and IL-13. Microglial death caused by butaprost occurred more quickly than that caused by LPS/IL-13; hence we selected different exposure times to measure microglial death in Fig. 2.

**ROS Mediate Death of Microglia Induced by LPS/IL-13 or EP2 Activation.** ROS have been reported to mediate cell death by apoptosis or programmed necrosis in different cell types (Hollensworth et al., 2000; Hou et al., 2005; Noguchi et al., 2008; Fortes et al., 2012; Bartlett et al., 2013; Won et al., 2013). Two ROS scavengers, NAC and BHA, were chosen to determine whether ROS is involved in microglial death induced by exposure to LPS/IL-13 or butaprost. NAC is a thiol precursor of L-cysteine and reduced glutathione. It is a source of sulfhydryl groups in cells and a scavenger of free radicals, interacting with ROS such as  $\bullet\text{OH}$  and  $\text{H}_2\text{O}_2$  (Aruoma et al., 1989). BHA, another well known ROS scavenger, can trap chain-carrying peroxy radicals (ROO) by donation of its phenolic hydrogen. Rat microglia were preincubated with NAC (1 or 10 mM) or BHA (1 or 10  $\mu\text{M}$ ) for 2 hours, followed by addition of LPS (10 ng/ml) plus IL-13 (20 ng/ml) for 6 days or followed by the EP2 agonist butaprost (200 nM) for 3 days. Microglia were stained with calcein-AM and the DNA intercalator Etd-1; cells were imaged and counted as either live or dead (Fig. 3A). Following treatment, NAC and BHA dose-dependently reduced microglial death induced by either LPS/IL-13 or butaprost (Fig. 3). This result indicates that ROS are involved in microglial death induced either by LPS/IL-13 or EP2 activation. Phase-contrast images were taken with a Zeiss Axio Observer A1 fluorescence microscope after the different treatments (Fig. 3E). Microglia in both the LPS and LPS/IL-13 groups initially became swollen and round compared with the typically elongated cells in the control condition; however, cell shrinkage was seen in the LPS/IL-13 group from day 3, suggesting apoptosis. Likewise, exposure to butaprost (2, 20, and especially 200 nM for 2 days) also caused microglia to shrink.

**With Carbon Monoxide Involved, the Antioxidant Hmox1 Opposes Microglial Death Induced by LPS/IL-13.** Hmox1 is a metabolic enzyme that utilizes NADPH and oxygen to break apart the heme moiety, liberating carbon monoxide (CO), iron, and biliverdin, which is subsequently converted to bilirubin (Fig. 4A). CO has profound effects on mitochondria, cellular respiration, and other hemoproteins to which it can bind; CO and bilirubin are both potent antioxidants. Sequestration of iron into ferritin and its recycling in the tissues is part of a homeodynamic process that controls oxidation-reduction in cellular metabolism. We confirmed (Liu et al., 2010) that LPS-induced Hmox1 expression is reduced by IL-13 (Supplemental Fig. 1A), and we also found that LPS-increased Hmox1 activity was reduced by IL-13, determined by measuring bilirubin production (Supplemental Fig. 1B). Live and dead cell assay was then performed to determine whether the replenishment of Hmox1 activity attenuated LPS/IL-13-induced microglial death. Microglia were incubated for 6 days with 10 ng/ml of LPS, 20 ng/ml of IL-13, and CoPP, a well known Hmox1 inducer (Cai et al., 2012). CoPP reduced LPS/IL-13-induced microglial death (Fig. 4B), indicating that microglial death is exacerbated by downregulation of Hmox1. Next, we examined which enzymatic product of Hmox1 was involved in protecting microglia from death. Microglia were exposed for 6 days to LPS, IL-13, and tricarbonyldichlororuthenium (II) dimer used as a source of CO (CORM) or bilirubin or  $\text{Fe}^{2+}$ ; then mortality was assessed. CORM but neither bilirubin nor  $\text{Fe}^{2+}$  caused a reduction in LPS/IL-13-induced microglial death (Fig. 4, C–E). These results indicate that the antioxidant Hmox1, with CO involved, opposes LPS/IL-13-induced microglial death.

**EP2 Signaling Increases Hmox1 Expression.** Based on results that LPS/IL-13-induced microglia death is mediated by EP2 activation but opposed by Hmox1, we explored the interaction between Hmox1 and EP2. First, microglia were exposed to LPS, IL-13, and either CORM, bilirubin, or  $\text{Fe}^{2+}$  for 3 days, and Western blot was performed to examine whether Hmox1's products influence IL-13-enhanced COX-2 expression.

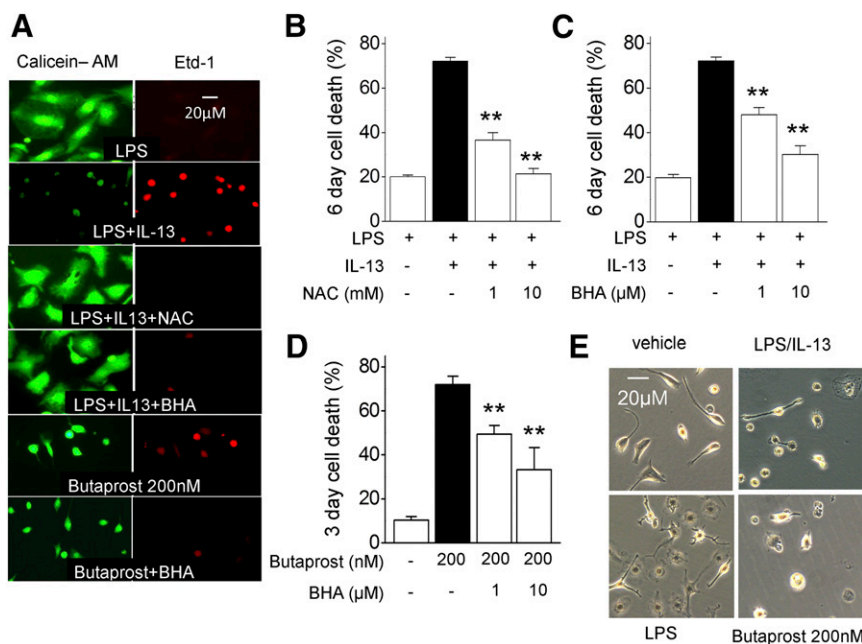


**Fig. 3.** ROS mediate microglial death induced by LPS/IL-13 or butaprost. Rat microglia were pre-treated with vehicle or ROS scavengers BHA or NAC for 2 hours followed by addition of 10 ng/ml of LPS and 20 ng/ml of IL-13 for 6 days (B and C) or 200 nM butaprost for 3 days (D). Cell death was measured by staining with calcein-AM and Etd-1. Representative images are shown. Data were analyzed by one-way analysis of variance with post hoc Bonferroni test. Data are shown as mean + S.E. (error bars);  $n = 3-6$ .  $**P < 0.01$  versus LPS/IL-13 or butaprost group. (E) Microglia were incubated with vehicle, 10 ng/ml of LPS, or 10 ng/ml of LPS plus 20 ng/ml of IL-13 for 4 days or 200 nM butaprost for 3 days, and phase-contrast images were taken with a Zeiss Axio Observer A1 fluorescence microscope. Representative images are shown;  $n = 6$ .

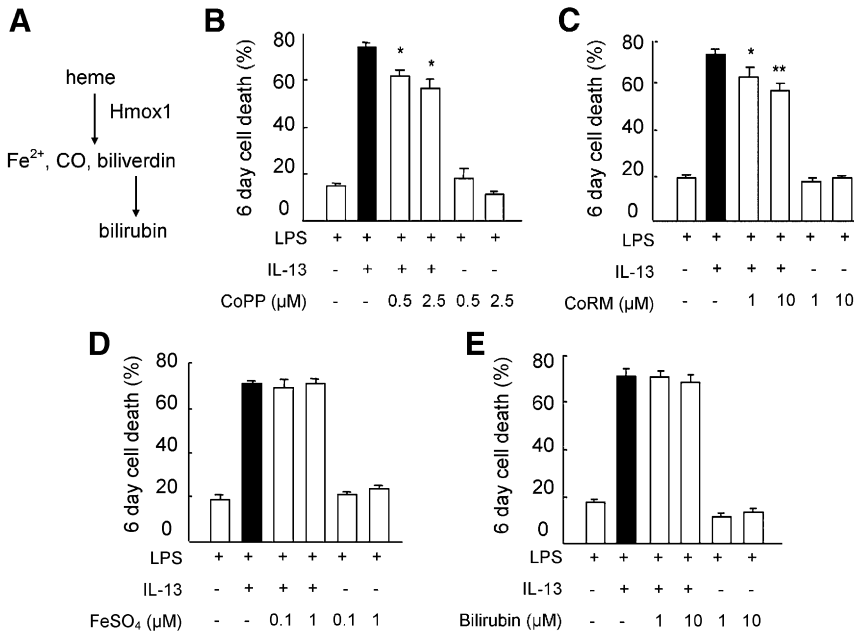


**Fig. 4.** Effects of Hmox1 inducer and its products on IL-13-induced death in activated rat microglia. (A) Hmox1 degrades heme into Fe<sup>2+</sup>, CO, and biliverdin, which is then converted to bilirubin. (B–E) Microglia were incubated with the Hmox1 inducer CoPP (B), tricarbonyldichlororuthenium (II) dimer used as a source of CO (CORM) (C), Fe<sup>2+</sup> (D), or bilirubin (E), together with 10 ng/ml of LPS and 20 ng/ml of IL-13 for 6 days. Cell death was evaluated by staining with calcein-AM and Etd-1. Data were analyzed by one-way analysis of variance with post hoc Bonferroni test. Data are shown as mean + S.E. (error bars); *n* = 6–8. \**P* < 0.05; \*\**P* < 0.01 versus LPS/IL-13 group.

Only CORM, which rescued microglia from LPS/IL-13-induced death (Fig. 4C), but not bilirubin or Fe<sup>2+</sup>, was found to reduce COX-2 expression dose-dependently (Supplemental Fig. 2). This result suggests that the downregulation of COX-2 by Hmox1's product CO might contribute to reduced microglial death.

To determine whether EP2 activation affects the expression of Hmox1, microglia were preincubated with the EP2 agonist butaprost (2 μM) for 1 hour, followed by addition of LPS (1 or 10 ng/ml) for 12 and 24 hours, and then mRNA and protein were isolated to measure Hmox1 expression. Interestingly, we found that butaprost potentiated induction of Hmox1 mRNA and protein by LPS, but butaprost alone was without effect (Fig. 5, A and B), indicating that EP2 activation increases Hmox1 expression in activated but not resting microglia. This result was further expanded in C57BL/6 mice that underwent pilocarpine-induced SE (Fig. 5, C and D). SE was allowed to proceed for 1 hour and then terminated by pentobarbital. Three hours later (i.e., 4 hours after SE onset), vehicle or TG6-10-1, which is a brain-permeant EP2 antagonist, was administered (5 mg/kg, i.p.). Two additional doses of TG6-10-1 were administered 21 and 30 hours after SE onset to approximately match the temporal pattern of COX-2 induction after pilocarpine (Jiang et al., 2015). One and 4 days after SE, groups of mice were sacrificed and hippocampal tissue was isolated to measure Hmox1 mRNA level. Hmox1 mRNA was increased both 1 and 4 days after SE, and TG6-10-1 treatment decreased Hmox1 mRNA expression at both time points (Fig. 5, C and D). These data indicate that EP2 activation increases Hmox1 expression both *in vitro* and *in vivo*, which could serve as a homeostatic mechanism in microglial activation.

**Role of Caspases 1 and 3 in Microglial Death Induced by LPS/IL-13 or Butaprost.** LPS/IL-13-induced microglial death was reported to have apoptotic characteristics—chromatin condensation and fragmentation and positive terminal deoxynucleotidyl transferase-mediated digoxigenin-deoxyuridine nick-end labeling staining (Yang et al., 2002). Interleukin-1-converting enzyme (caspase-1), which is an enzyme that cleaves the precursor forms of the inflammatory cytokines IL-1β and IL-18 into active mature peptides, is one component of the

inflammasome that triggers pyroptosis. Pyroptosis is a form of programmed cell death initially associated with antimicrobial responses during inflammation (Aachoui et al., 2013). During pyroptosis, cells swell, eventually lyse, and release proinflammatory mediators. Caspase-1 can also promote apoptosis (Sarkar et al., 2006; Exline et al., 2014; Sollberger et al., 2015). We examined whether caspase-1 is involved in LPS/IL-13-induced microglial death. Rat microglia were preincubated with caspase-1 inhibitors Z-WEHD-FMK (20 μM) or Ac-YVAD-cmk (50 μM) for 4 hours, followed by addition of LPS/IL-13 for 6 days. Microglia were stained with calcein-AM and Etd-1, and cells were imaged and counted. Both Z-WEHD-FMK and Ac-YVAD-cmk greatly reduced microglial death (Fig. 6A), suggesting that caspase-1 is largely responsible for LPS/IL-13-induced microglial death. Z-WEHD-FMK also nearly eliminated microglial death induced by a low concentration (2 nM) of butaprost, but had no effect on death caused by 200 or 2000 nM butaprost (Fig. 6B). Butaprost (2–2000 nM) induced the formation of activated caspase-3 (Fig. 6C), which is one of the key caspases responsible for cleavage of numerous cellular proteins, leading to the biochemical and morphologic hallmarks of apoptosis (Brancolini et al., 1997). These results, taken together, suggest two modes of microglial death, pyroptosis at low levels of EP2 activation and predominantly apoptosis as EP2 activation increases.

**EP2 Activation Reduces Levels of Both Pro-caspase-1 and Pro-IL-1β Proteins.** Because inhibitors of both EP2 and caspase-1 can nearly fully prevent LPS/IL-13-induced microglial death, we explored whether the EP2 agonist leads to caspase-1 activation, which cleaves pro-IL-1β into mature IL-1β. Primary rat microglia were preincubated with 2 μM butaprost for 1 hour, followed by addition of LPS (10 ng/ml) for 12 and 24 hours, and then protein was isolated to analyze caspase-1 and IL-1β expression. Both procaspase-1 and pro-IL-1β were increased by LPS, and interestingly, both were decreased by the addition of butaprost (Fig. 7, A and C). However, neither mature caspase-1 nor mature IL-1β protein was detected (not shown). When microglia were preincubated with LPS (10 ng/ml) for 6 hours followed by addition of 2 μM butaprost for indicated times, Western blot showed that

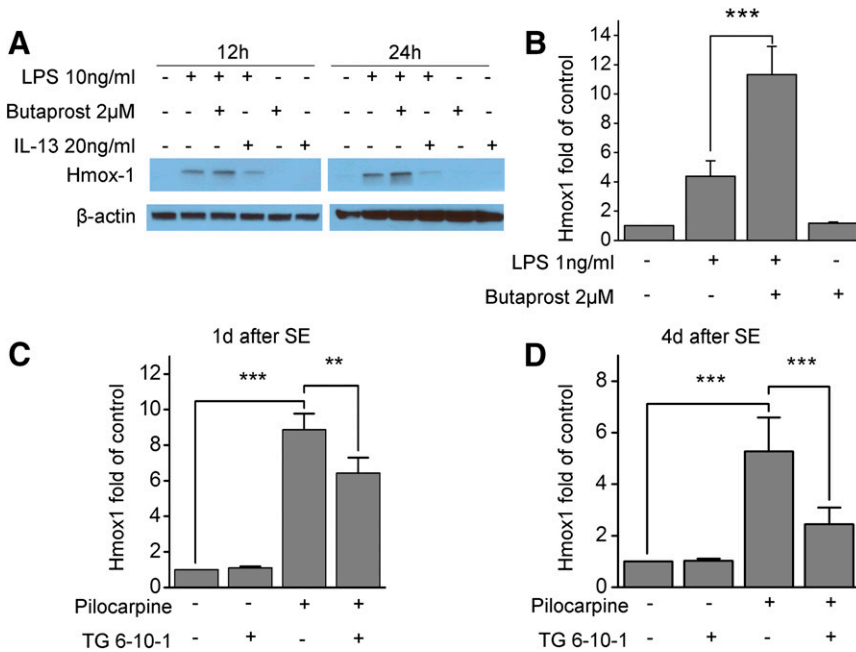


**Fig. 5.** EP2 activation increases Hmox-1 expression. Rat microglia were pretreated with the EP2 agonist butaprost for 1 hour, followed by addition of 1 or 10 ng/ml of LPS for 12 and 24 hours. Cells were lysed to obtain total protein samples for Western blot and mRNA samples for qRT-PCR. (A) The changes in Hmox1 protein induced 12 and 24 hours after addition of 10 ng/ml of LPS. The data shown are representative of three independent experiments. (B) The changes in Hmox1 mRNA 12 hours after addition of 1 ng/ml of LPS ( $n = 5$ ). (C and D) The changes in Hmox1 mRNA in mouse hippocampi 1 day (C) and 4 days (D) after SE measured by qRT-PCR ( $n = 6-8$ ). Data were analyzed by one-way analysis of variance with post hoc Bonferroni test. Data are shown as mean + S.E. (error bars). \*\* $P < 0.01$ ; \*\*\* $P < 0.001$ .

butaprost time-dependently reduced LPS-enhanced pro-IL-1 $\beta$  expression (Fig. 7B), although, again, no mature IL-1 $\beta$  was detected. By contrast, butaprost increased the mRNA levels of both IL-1 $\beta$  (Quan et al., 2013) and caspase-1 in activated microglia (Fig. 7D).

### Discussion

The major findings of this study are that 1) EP2 signaling regulates the death of activated microglia; 2) cell death mediated by EP2 involves the activation of caspases 1 and 3 as well as the generation of ROS; and 3) both activated microglia and EP2 activation engage an antioxidant Hmox1 pathway

that opposes cell death. Microglial death induced by LPS plus IL-13 was potentiated by butaprost and fully prevented by EP2 antagonists. Inhibition of caspase-1 could also fully prevent the death of activated microglia produced by IL-13 or weak EP2 activation by 2 nM butaprost, but interestingly, caspase-1 inhibitors were ineffective against microglial death induced by strong EP2 activation. By contrast, EP2 activation by butaprost also caused a slowly developing apoptosis in resting microglia characterized by cell shrinkage and increased caspase-3 cleavage. Butaprost reduced the expression of procaspase-1 and pro-IL-1 $\beta$  proteins in activated microglia while increasing their mRNA levels, which is consistent with the possibility that EP2 activation induces the formation of

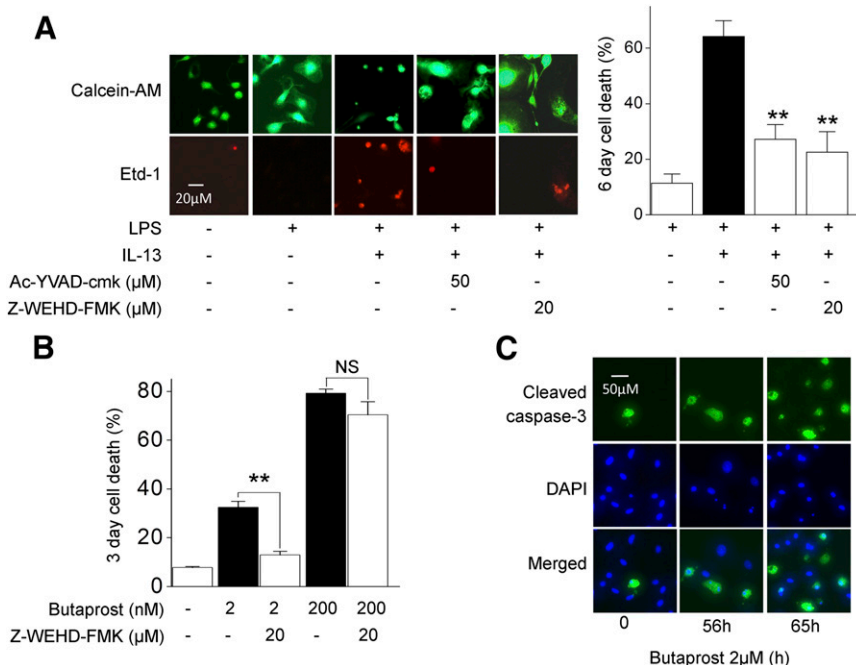


**Fig. 6.** Involvement of caspases 1 and 3 in microglial death caused by LPS/IL-13 or butaprost. (A) Rat microglia were pretreated with vehicle or caspase-1 inhibitors Ac-YVAD-cmk or Z-WEHD-FMK for 4 hours, followed by addition of 10 ng/ml of LPS and 20 ng/ml of IL-13 for 6 days. Cell death was determined by staining with calcein-AM and Etd-1. Representative images are shown. Data were analyzed by one-way analysis of variance (ANOVA) with Dunnett's test. Data are expressed as mean + S.E. (error bars);  $n = 4-6$ . \*\* $P < 0.01$  versus control. (B) Microglia were incubated with the indicated concentrations of butaprost and the caspase-1 inhibitor for 3 days and microglial death assessed by the live and dead cell assay. Data are shown as mean + S.E.;  $n = 3$ . \*\* $P < 0.01$  by one-way ANOVA with post-hoc Bonferroni test. (C) Rat microglia were incubated with vehicle or 2 μM butaprost for indicated times. Microglia were fixed and stained for cleaved caspase-3 and nucleic acid (DAPI). Representative images are shown;  $n = 3$ . NS, not significant.

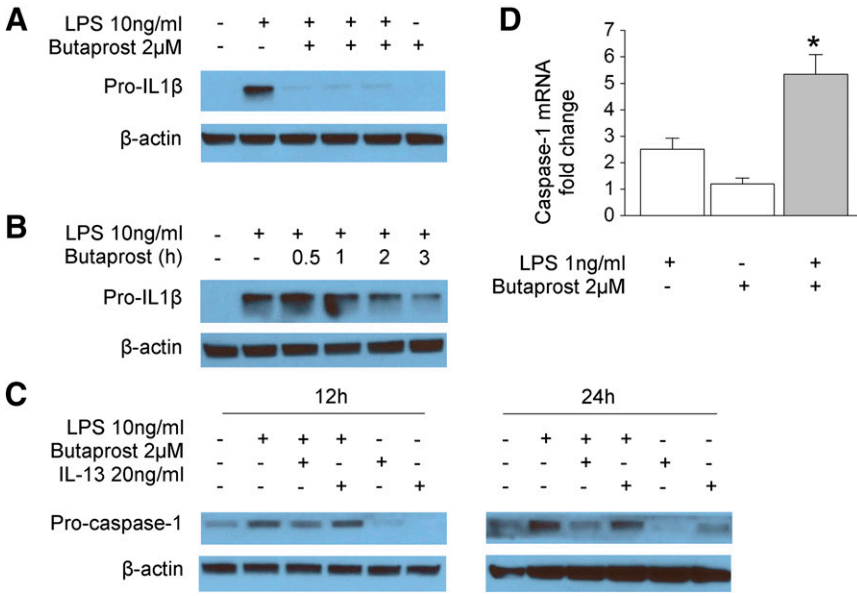


**Fig. 7.** Effect of EP2 activation on inflammasome signaling. Rat microglia were pretreated with 2 μM butaprost for 1 hour, followed by 10 ng/ml of LPS for 12 and 24 hours, or microglia were incubated with 10 ng/ml of LPS for 6 hours, followed by 2 μM butaprost for 0.5–3 hours. Cells were lysed to obtain protein samples for Western blot. (A and B) The changes in pro-IL-1β protein induced 12 hours after LPS; no mature IL-1β was detected under any condition (not shown). (C) Changes in procaspase-1 protein induced 12 and 24 hours after LPS and butaprost; no mature caspase-1 was detected. These data are representative of three independent experiments. (C) and Fig. 5A were from the same blot that was stripped and reblotted, so the β-actin loading controls are reproduced. (D) Microglia were pretreated with 2 μM butaprost, followed by addition of 1 ng/ml of LPS for 12 hours, and caspase-1 mRNA level was measured by qRT-PCR. The mRNA changes were normalized to the mean of the control group. Data were analyzed by one-sample *t* test with Bonferroni correction. Data are expressed as mean + S.E. (error bars); *n* = 5. \**P* < 0.05 versus LPS group.

mature caspase-1 and IL-1β. A schematic diagram (Fig. 8) shows a pro-death pathway initiated by Toll-like receptor 4 activation involving COX-2 and EP2, which is opposed by a feedback/feedforward antioxidant pathway mediated by Hmox1 and its enzymatic product, CO. We propose that low levels of EP2 activation triggered by LPS plus IL-13 engage mainly a caspase-1 death pathway, whereas this pyroptotic pathway is overridden by apoptosis potentially mediated by caspase-3 during strong EP2 activation (Fig. 8). This situation is similar to the differential effect of low versus high *N*-methyl-D-aspartate receptor activation on two modes of neuronal death (Bonfoco et al., 1995).

EP2 receptors play an essential role in the regulation of inflammatory cytokine and chemokine expression in many different cell types, including macrophages, microglia, and tumor cells (Jiang and Dingleline, 2013; Johansson et al., 2013). Examining both resting and LPS-activated microglia, we found that rat primary microglia upregulate their EP2 receptors with a 4-fold increase in mRNA level and an 8-fold increase in agonist potency (Fig. 1). This result is different from our previous finding that the potency of EP2 receptors in rat microglia was similar between resting and activated states (Quan et al., 2013). These two findings can potentially be reconciled by different culture conditions—here we included 10% FBS but no GM-CSF in the media after cell plating. By enhancing the expression and potency of EP2

receptors upon insults, microglia can actively engage themselves in regulating critical inflammatory pathways with amplified signaling downstream of EP2 receptors. EP2 levels in vivo can also be dynamically regulated. The EP2 mRNA level in mouse hippocampus was increased 3- to 4-fold within 16 hours of SE and was associated with a strong inflammatory response, although bulk EP2 protein levels were unchanged (Jiang et al., 2015). EP2 mediates proinflammatory effects in models of innate immunity (Ganesh et al., 2013), Alzheimer’s disease (Johansson et al., 2015), amyotrophic lateral sclerosis (Liang et al., 2008), and SE (Jiang et al., 2012, 2013; Varvel et al., 2015). EP2 receptor antagonists quench neuroinflammation after SE (Jiang et al., 2012, 2013). Whether EP2 agonist potency itself is increased in these disease models and thus contributes to disease progression is an interesting question.

Death of activated microglia is one potential mechanism for resolution of inflammation. IL-13 promotes the death of LPS-activated microglia characterized by positive terminal deoxynucleotidyl transferase-mediated digoxigenin-deoxyuridine nick-end labeling staining and DNA fragmentation (Yang et al., 2002), together with caspase-12-mediated endoplasmic reticulum stress (Szegezdi et al., 2003; Liu et al., 2010), suggesting an apoptotic mode of microglial death. We found that microglial death induced by LPS/IL-13 was blocked by two caspase-1 inhibitors (Fig. 6, A and B). The activation of

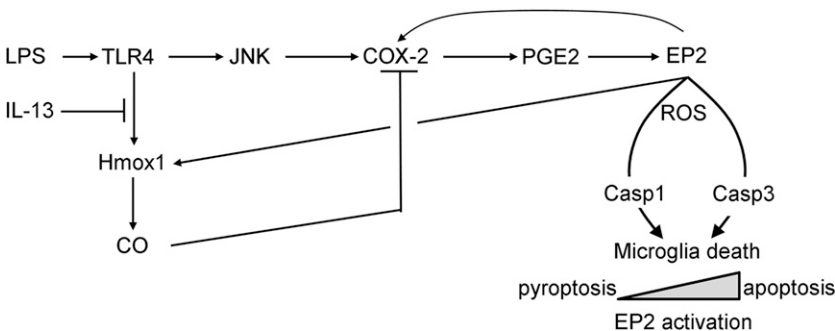


**Fig. 8.** Proposed role of EP2 and Hmox1 in death of activated microglia. The proposed pathways are deduced from the current results as well as results presented in Yang et al. (2002). JNK, Jun kinase; TLR, Toll-like receptor.



caspase-1 is a key feature of inflammasome formation, which results in subsequent processing of IL-1 $\beta$  and IL-18 and can induce an inflammatory, lytic type of cell death known as pyroptosis. However, recent studies show that caspase-1 can also be involved in apoptosis. After intraperitoneal challenge of mice with live *Escherichia coli*, splenic B-lymphocyte apoptosis was found in wild-type mice and both IL-1 $\beta$  knockout and IL-1 $\beta$ /IL-18 double-knockout mice but not in caspase-1 knockout mice. Importantly, IL-1 $\beta$ /IL-18 double-knockout mice were protected from splenic cell apoptosis by the pan-caspase inhibitor z-VAD-fmk (Sarkar et al., 2006). The caspase-1 inhibitor YVAD-cmk reduced human lymphocyte apoptosis in sepsis (Exline et al., 2014). The induction of caspase-1 precedes that of caspase-3 in UVB-stimulated human keratinocytes, and cells with reduced caspase-1 expression show much less caspase-3-associated apoptosis (Sollberger et al., 2015). All these findings indicate that under certain conditions caspase-1 can induce caspase-3 activation, which can trigger subsequent apoptosis.

EP2 activation caused a mixed immune state in classically activated microglia, exacerbating the rapid induction of some proinflammatory mediators (COX-2, IL-6, and IL-1 $\beta$ ) while blunting others (tumor necrosis factor- $\alpha$ , CCL3, and CCL4), and thus EP2 regulates microglial activation (Quan et al., 2013). We confirmed the finding of Yang et al. (2006) that EP2 activation also dose-dependently induces the death of resting microglia, and we show here that activation of both EP2 receptors and caspase-1 underlies the death of microglia caused by IL-13 (Fig. 2B; Fig. 6, A and B). In addition, butaprost can induce an apoptotic morphology of resting microglia, accompanied by increased caspase-3 cleavage (Fig. 6D) as well as DNA fragmentation and poly (ADP-ribose) polymerase cleavage (Nagano et al., 2014). The death of microglia caused by high concentrations of butaprost is dependent upon ROS (Fig. 3D) and is completely blocked by an EP2 antagonist (Fig. 2F). In LPS-activated microglia, butaprost increases caspase-1 and IL-1 $\beta$  mRNA expression while reducing the protein levels of both procaspase-1 and pro-IL-1 $\beta$ , consistent with the possibility that EP2 activation induces the formation of mature caspase-1 and IL-1 $\beta$  from their precursor. However, we were not able to detect mature caspase-1 or IL-1 $\beta$  by Western blot and suspect that the mature forms were quickly degraded in our culture conditions. We propose that strong EP2 activation in resting microglia activates caspase-3 directly and produces apoptosis. By contrast, in LPS-activated microglia with upregulated EP2 receptors, weaker EP2 activation induces caspase-1 signaling, which then promotes pyroptosis or caspase-3 cleavage, leading to apoptosis (Fig. 8). At the same time, EP2 activation by butaprost exerts a negative feedback role by enhancing Hmx1 expression both in vitro and in vivo (Fig. 5, A–D), which opposes activated microglia death (Fig. 4, B and C). Taken together, our results indicate that EP2 activation initially promotes microglial activation and then induces slow death by either pyroptosis or apoptosis. These conclusions are drawn from the effects of selective EP2 agonists and antagonists, and it would be worthwhile to confirm with microglia deficient in EP2 receptors (Johansson et al., 2013).

Considering the crucial role of EP2 signaling in regulating classic activation of microglia (Quan et al., 2013), we conclude that COX-2-dependent EP2 activation promotes microglial activation in early stages of inflammation and then causes

a delayed death of activated microglia. Thus, as suggested by Yang et al. (2002), microglial death could be one event underlying the resolution of neuroinflammation. Targeting EP2 signaling pathways may be an efficient approach to control the degree of microglial activation, thus reducing chronic inflammation and brain damage in neurologic diseases. The therapeutic window for EP2 antagonists opens after seizures with the neuronal induction of COX-2 and consequent production of PGE<sub>2</sub> (Jiang et al., 2015; Rojas et al., 2015). Our data suggest that the therapeutic window might close toward the end of active inflammation, when microglial death is needed to resolve inflammation.

#### Acknowledgments

The authors thank Ashebo Rojas, Nicholas Varvel, and Nadia Lelutiu for help and advice.

#### Authorship Contributions

Participated in research design: Fu, Yang, Joe, Dingledine.

Conducted experiments: Fu, Yang, Jiang.

Performed data analysis: Fu, Yang, Dingledine.

Wrote or contributed to the writing of the manuscript: Fu, Yang, Jiang, Ganesh, Dingledine.

#### References

- Aachoui Y, Sagulenko V, Miao EA, and Stacey KJ (2013) Inflammasome-mediated pyroptotic and apoptotic cell death, and defense against infection. *Curr Opin Microbiol* **16**:319–326.
- Aruoma OI, Halliwell B, Hoey BM, and Butler J (1989) The antioxidant action of N-acetylcysteine: its reaction with hydrogen peroxide, hydroxyl radical, superoxide, and hypochlorous acid. *Free Radic Biol Med* **6**:593–597.
- Bartlett R, Yerbury JJ, and Sluyter R (2013) P2X7 receptor activation induces reactive oxygen species formation and cell death in murine EOC13 microglia. *Mediators Inflamm* **2013**:271813.
- Bonfoco E, Krainc D, Ankarcrona M, Nicotera P, and Lipton SA (1995) Apoptosis and necrosis: two distinct events induced, respectively, by mild and intense insults with N-methyl-D-aspartate or nitric oxide/superoxide in cortical cell cultures. *Proc Natl Acad Sci USA* **92**:7162–7166.
- Borges K, Gearing M, McDermott DL, Smith AB, Almonte AG, Wainer BH, and Dingledine R (2003) Neuronal and glial pathological changes during epileptogenesis in the mouse pilocarpine model. *Exp Neurol* **182**:21–34.
- Brancolini C, Lazarevic D, Rodriguez J, and Schneider C (1997) Dismantling cell-cell contacts during apoptosis is coupled to a caspase-dependent proteolytic cleavage of beta-catenin. *J Cell Biol* **139**:759–771.
- Caggiano AO and Kraig RP (1999) Prostaglandin E receptor subtypes in cultured rat microglia and their role in reducing lipopolysaccharide-induced interleukin-1 $\beta$  production. *J Neurochem* **72**:565–575.
- Cai C, Teng L, Vu D, He JQ, Guo Y, Li Q, Tang XL, Rokosh G, Bhatnagar A, and Bolli R (2012) The heme oxygenase 1 inducer (CoPP) protects human cardiac stem cells against apoptosis through activation of the extracellular signal-regulated kinase (ERK)/NRF2 signaling pathway and cytokine release. *J Biol Chem* **287**:33720–33732.
- Chu CH, Chen SH, Wang Q, Langenbach R, Li H, Zeldin D, Chen SL, Wang S, Gao H, and Lu RB et al. (2014) PGE2 inhibits IL-10 production via EP2-mediated  $\beta$ -arrestin signaling in neuroinflammatory condition. *Mol Neurobiol* DOI: 10.1007/s12035-014-8889-0 [published ahead of print].
- Deveraux QL, Takahashi R, Salvesen GS, and Reed JC (1997) X-linked IAP is a direct inhibitor of cell-death proteases. *Nature* **388**:300–304.
- Exline MC, Justiniano S, Hollyfield JL, Berhe F, Besecker BY, Das S, Wewers MD, and Sarkar A (2014) Microvesicular caspase-1 mediates lymphocyte apoptosis in sepsis. *PLoS One* **9**:e90968.
- Fortes GB, Alves LS, de Oliveira R, Dutra FF, Rodrigues D, Fernandez PL, Souto-Padron T, De Rosa MJ, Kelliher M, and Golenbock D et al. (2012) Heme induces programmed necrosis on macrophages through autocrine TNF and ROS production. *Blood* **119**:2368–2375.
- Ganesh T, Jiang J, Shashidharamurthy R, and Dingledine R (2013) Discovery and characterization of carbamothioylacrylamides as EP2 selective antagonists. *ACS Med Chem Lett* **4**:616–621.
- Ganesh T, Jiang J, and Dingledine R (2014a) Development of second generation EP2 antagonists with high selectivity. *Eur J Med Chem* **82**:521–535.
- Ganesh T, Jiang J, Yang MS, and Dingledine R (2014b) Lead optimization studies of cinnamic amide EP2 antagonists. *J Med Chem* **57**:4173–4184.
- Hallinan EA, Hagen TJ, Tsymbalov S, Husa RK, Lee AC, Stapelfeld A, and Savage MA (1996) Aminoacetyl moiety as a potential surrogate for diacylhydrazine group of SC-51089, a potent PGE2 antagonist, and its analogs. *J Med Chem* **39**:609–613.
- Hollensworth SB, Shen C, Sim JE, Spitz DR, Wilson GL, and LeDoux SP (2000) Glial cell type-specific responses to menadione-induced oxidative stress. *Free Radic Biol Med* **28**:1161–1174.
- Hou RC, Wu CC, Huang JR, Chen YS, and Jeng KC (2005) Oxidative toxicity in BV-2 microglia cells: sesamol neuroprotection of H2O2 injury involving activation of p38 mitogen-activated protein kinase. *Ann N Y Acad Sci* **1042**:279–285.

- Jiang J and Dingleline R (2013) Role of prostaglandin receptor EP2 in the regulations of cancer cell proliferation, invasion, and inflammation. *J Pharmacol Exp Ther* **344**:360–367.
- Jiang J, Ganesh T, Du Y, Quan Y, Serrano G, Qui M, Speigel I, Rojas A, Lelutiu N, and Dingleline R (2012) Small molecule antagonist reveals seizure-induced mediation of neuronal injury by prostaglandin E2 receptor subtype EP2. *Proc Natl Acad Sci USA* **109**:3149–3154.
- Jiang J, Ganesh T, Du Y, Thepchatri P, Rojas A, Lewis I, Kurtkaya S, Li L, Qui M, and Serrano G et al. (2010) Neuroprotection by selective allosteric potentiators of the EP2 prostaglandin receptor. *Proc Natl Acad Sci USA* **107**:2307–2312.
- Jiang J, Quan Y, Ganesh T, Pouliot WA, Dudek FE, and Dingleline R (2013) Inhibition of the prostaglandin receptor EP2 following status epilepticus reduces delayed mortality and brain inflammation. *Proc Natl Acad Sci USA* **110**:3591–3596.
- Jiang J, Yang MS, Quan Y, Gueorguieva P, Ganesh T, and Dingleline R (2015) Therapeutic window for cyclooxygenase-2 related anti-inflammatory therapy after status epilepticus. *Neurobiol Dis* DOI: 10.1016/j.nbd.2014.12.032 [published ahead of print].
- Johansson JU, Pradhan S, Lokteva LA, Woodling NS, Ko N, Brown HD, Wang Q, Loh C, Cekanaviciute E, and Buckwalter M et al. (2013) Suppression of inflammation with conditional deletion of the prostaglandin E2 EP2 receptor in macrophages and brain microglia. *J Neurosci* **33**:16016–16032.
- Johansson JU, Woodling NS, Wang Q, Panchal M, Liang X, Trueba-Saiz A, Brown HD, Mhatre SD, Loui T, and Andreasson KI (2015) Prostaglandin signaling suppresses beneficial microglial function in Alzheimer's disease models. *J Clin Invest* **125**:350–364.
- Jung DY, Lee H, Jung BY, Ock J, Lee MS, Lee WH, and Suk K (2005) TLR4, but not TLR2, signals autoregulatory apoptosis of cultured microglia: a critical role of IFN-beta as a decision maker. *J Immunol* **174**:6467–6476.
- Kiriyama M, Ushikubi F, Kobayashi T, Hirata M, Sugimoto Y, and Narumiya S (1997) Ligand binding specificities of the eight types and subtypes of the mouse prostanoid receptors expressed in Chinese hamster ovary cells. *Br J Pharmacol* **122**:217–224.
- Kutty RK and Maines MD (1982) Oxidation of heme c derivatives by purified heme oxygenase. Evidence for the presence of one molecular species of heme oxygenase in the rat liver. *J Biol Chem* **257**:9944–9952.
- Liang X, Wang Q, Shi J, Lokteva L, Breyer RM, Montine TJ, and Andreasson K (2008) The prostaglandin E2 EP2 receptor accelerates disease progression and inflammation in a model of amyotrophic lateral sclerosis. *Ann Neurol* **64**:304–314.
- Liu SH, Yang CN, Pan HC, Sung YJ, Liao KK, Chen WB, Lin WZ, and Sheu ML (2010) IL-13 downregulates PPAR-gamma/heme oxygenase-1 via ER stress-stimulated calpain activation: aggravation of activated microglia death. *Cell Mol Life Sci* **67**:1465–1476.
- Marriott HM, Hellewell PG, Cross SS, Ince PG, Whyte MK, and Dockrell DH (2006) Decreased alveolar macrophage apoptosis is associated with increased pulmonary inflammation in a murine model of pneumococcal pneumonia. *J Immunol* **177**:6480–6488.
- Murakami M, Naraba H, Tanioka T, Semmyo N, Nakatani Y, Kojima F, Ikeda T, Fueki M, Ueno A, and Oh S et al. (2000) Regulation of prostaglandin E2 biosynthesis by inducible membrane-associated prostaglandin E2 synthase that acts in concert with cyclooxygenase-2. *J Biol Chem* **275**:32783–32792.
- Nagano T, Kimura SH, and Takemura M (2014) Prostaglandin E2 induces apoptosis in cultured rat microglia. *Brain Res* **1568**:1–9.
- Narumiya S, Sugimoto Y, and Ushikubi F (1999) Prostanoid receptors: structures, properties, and functions. *Physiol Rev* **79**:1193–1226.
- Noguchi T, Ishii K, Fukutomi H, Naguro I, Matsuzawa A, Takeda K, and Ichijo H (2008) Requirement of reactive oxygen species-dependent activation of ASK1-p38 MAPK pathway for extracellular ATP-induced apoptosis in macrophage. *J Biol Chem* **283**:7657–7665.
- Quan Y, Jiang J, and Dingleline R (2013) EP2 receptor signaling pathways regulate classical activation of microglia. *J Biol Chem* **288**:9293–9302.
- Ransohoff RM and Cardona AE (2010) The myeloid cells of the central nervous system parenchyma. *Nature* **468**:253–262.
- Rojas A, Ganesh T, Lelutiu N, Gueorguieva P, and Dingleline R (2015) Inhibition of the prostaglandin EP2 receptor is neuroprotective and accelerates functional recovery in a rat model of organophosphorus induced status epilepticus. *Neuropharmacology* **93C**:15–27.
- Sarkar A, Hall MW, Exline M, Hart J, Knatz N, Gatson NT, and Wewers MD (2006) Caspase-1 regulates Escherichia coli sepsis and splenic B cell apoptosis independently of interleukin-1beta and interleukin-18. *Am J Respir Crit Care Med* **174**:1003–1010.
- Shi J, Johansson J, Woodling NS, Wang Q, Montine TJ, and Andreasson K (2010) The prostaglandin E2 E-prostanoid 4 receptor exerts anti-inflammatory effects in brain innate immunity. *J Immunol* **184**:7207–7218.
- Shin WH, Lee DY, Park KW, Kim SU, Yang MS, Joe EH, and Jin BK (2004) Microglia expressing interleukin-13 undergo cell death and contribute to neuronal survival in vivo. *Glia* **46**:142–152.
- Sollberger G, Strittmatter GE, Grossi S, Garstkiewicz M, Auf dem Keller U, French LE, and Beer HD (2015) Caspase-1 activity is required for UVB-induced apoptosis of human keratinocytes. *J Invest Dermatol* DOI: 10.1038/jid.2014.551 [published ahead of print].
- Szegezdi E, Fitzgerald U, and Samali A (2003) Caspase-12 and ER-stress-mediated apoptosis: the story so far. *Ann N Y Acad Sci* **1010**:186–194.
- Van Dyken SJ and Locksley RM (2013) Interleukin-4- and interleukin-13-mediated alternatively activated macrophages: roles in homeostasis and disease. *Annu Rev Immunol* **31**:317–343.
- Varvel NH, Jiang J, and Dingleline R (2015) Candidate drug targets for prevention or modification of epilepsy. *Annu Rev Pharmacol Toxicol* **55**:229–247.
- Watanabe K, Kawamori T, Nakatsugi S, Ohta T, Ohuchida S, Yamamoto H, Maruyama T, Kondo K, Ushikubi F, and Narumiya S et al. (1999) Role of the prostaglandin E receptor subtype EP1 in colon carcinogenesis. *Cancer Res* **59**:5093–5096.
- Won SY, Kim SR, Maeng S, and Jin BK (2013) Interleukin-13/Interleukin-4-induced oxidative stress contributes to death of prothrombin-2 (pKr-2)-activated microglia. *J Neuroimmunol* **265**:36–42.
- Yang MS, Ji KA, Jeon SB, Jin BK, Kim SU, Jou I, and Joe E (2006) Interleukin-13 enhances cyclooxygenase-2 expression in activated rat brain microglia: implications for death of activated microglia. *J Immunol* **177**:1323–1329.
- Yang MS, Park EJ, Sohn S, Kwon HJ, Shin WH, Pyo HK, Jin B, Choi KS, Jou I, and Joe EH (2002) Interleukin-13 and -4 induce death of activated microglia. *Glia* **38**:273–280.

---

**Address correspondence to:** Yujiao Fu, Department of Pharmacology, Emory University School of Medicine, 5001 Rollins Research Center, 1510 Clifton Road, Atlanta, GA 30322. E-mail: yujiao.fu@gmail.com

---